

Investigation of Flange Local Bending Under Flexible Patch Loading

LYLE P. CARDEN, GOKHAN PEKCAN and AHMAD M. ITANI

When a rigid patch or line load is applied to a beam, the flange is only able to deform as allowed by deformation of the web, thus the capacity of the web controls the design. However, in applications where a patch load is flexible, it is possible for the flange to bend around the web, which may limit the capacity of the beam. A flexible patch load is considered one where the load is able to deform as the loaded member deforms, resulting in a more uniform distribution of applied stress than when a load is applied through a rigid element. A recent study by the authors (Carden, Pekcan and Itani, 2005) has shown that flange bending may be the critical limit state in applications such as bridge falsework where timber posts bear on unstiffened steel beams. The resulting damage mechanism illustrated in Figure 1 has the potential to lead to instabilities and collapse of bridge falsework during construction.

Past studies on the effect of patch loading (Roberts and Rockey, 1979; Roberts and Markovic, 1983; Elgaaly, 1983; Roberts and Newark, 1997; Shahabian and Roberts, 1999; Graciano and Edlund, 2003) have generally assumed rigid patch loads which have not resulted in flange bending other than that required for deformation of the web. The case of a flexible patch load provided by a timber post has not been considered, thus there is currently no design methodology to assess flange bending capacity under this loading condition.

The AISC *Specification for Structural Steel Buildings* (AISC, 2005), hereafter referred to as the AISC *Specification*, allows for the calculation of flange bending capacity in beam-column joints. The ultimate flange bending capacity

in the column flange assumes that a tensile line load is applied to the column flange from the beam flange. A yield line pattern in the column flange and a uniform stress distribution from the beam flange is assumed in order to derive an equation to calculate the ultimate capacity of the flange (Graham, Sherbourne and Khabbaz, 1959). However, this equation, which is based on the need to limit tensile stresses in the connection of the beam flange at the column web, is conservative if applied to a compressive patch load. The conservatism is in part because a patch load is able to engage a larger region in resisting bending of the flange than a linearly applied load from an adjoining flange. In addition weld fracture is not the concern resulting from flange bending in this application.

Two methods that account for the effect of patch loading from timber and steel posts on beams were developed elsewhere (Carden et al., 2005) and are summarized in what follows. In the first, the interaction between the flange bending capacity and the post compression capacity was considered. If the flange is significantly weaker than the post, it will tend to dictate the strength of the joint region. On the other hand,

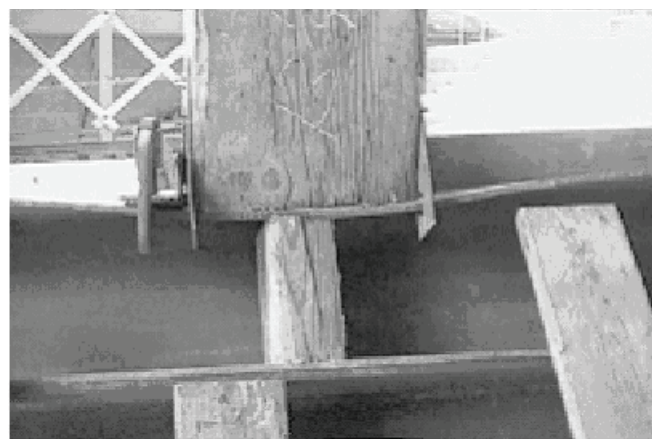


Fig. 1. Flange bending in sill beam (courtesy of J. Lammers, Caltrans).

Lyle P. Carden is a structural engineer, Martin & Chock, Inc., Honolulu, HI.

Gokhan Pekcan is assistant professor, department of civil and environmental engineering, University of Nevada, Reno, NV.

Ahmad M. Itani is professor, department of civil and environmental engineering, University of Nevada, Reno, NV.

if the post compression strength is notably lower than the beam flange capacity then the post will dictate the overall response. If the flange and post have similar strengths then the joint capacity will tend to be smaller than the capacity of either component. The second method uses an effective bearing area for the post, which accounts for flange bending capacity in a secondary manner by reducing the effective area of the post depending on the thickness of the flange. The first method was found to be most effective for predicting the flange-post bearing joint strength with a timber post; however, with a steel post, which is axially rigid, the second method leads to more accurate assessment of the joint strength.

The above methods were developed assuming a concentric loading, without the use of any blocking, which is sometimes used in attempts to strengthen the joint region. This paper describes a series of experiments and finite element analyses to investigate the effectiveness of the above methodologies for predicting the flange-post joint capacity; considering eccentricities between the centroids of the beam and post, and the use of blocking. The methodologies are then developed into a form appropriate for design using load and resistance factor design (LRFD) and allowable stress design (ASD) procedures.

FLANGE-POST CAPACITY

Interaction Method

The flange bending capacity, R_f , due to a flexible patch load similar to that associated with bearing of a timber post can be described as

$$R_f = \beta t_f^2 F_{yf} \quad (1)$$

where

β = a constant determined from a yield line analysis (Carden et al., 2005)

t_f = thickness of the flange

F_{yf} = specified minimum yield stress of the flange

Expressions for β were developed assuming a uniform and triangular stress distribution for the patch load, as shown in Figure 2. However, for a nominal 12 × 12 in. post, a β value equal to 18 was found to be appropriate for calculating the flange bending capacity for a range of beams with flange thicknesses between 0.44 and 0.94 in. subjected to concentric patch loading.

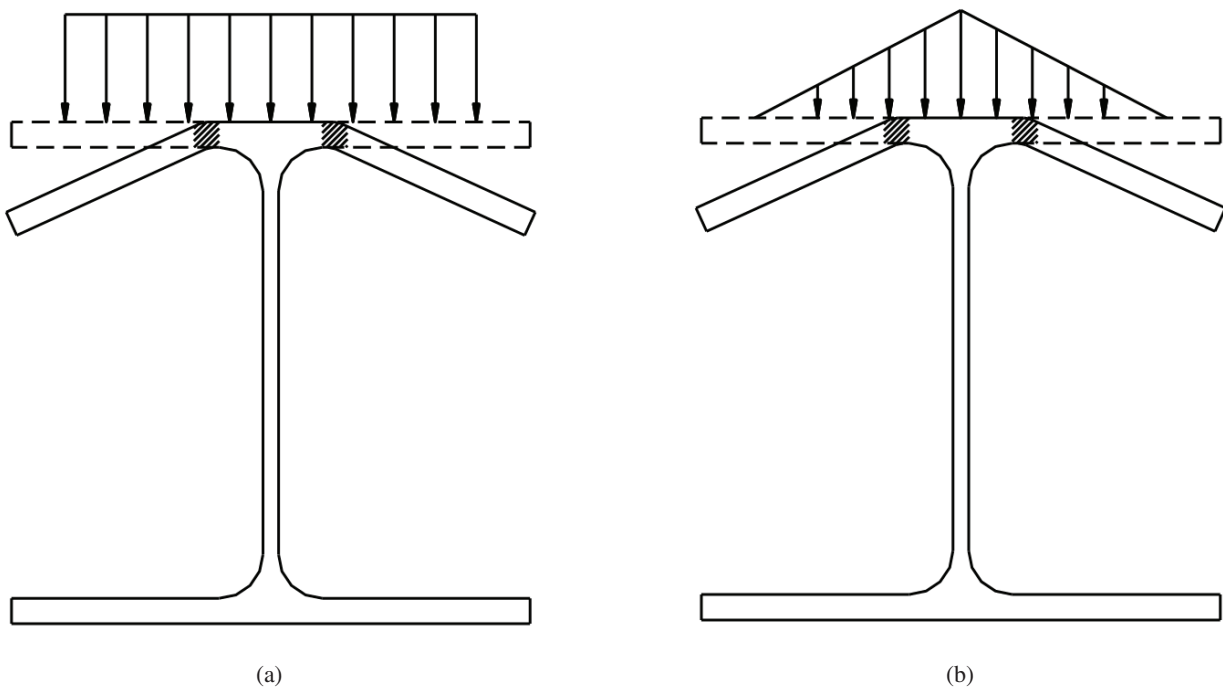


Fig. 2. Patch load assuming: (a) a uniform stress distribution and (b) a triangular stress distribution.

In order to calculate the capacity of the flange-post bearing region it is also necessary to consider the compression capacity of a short timber post which is given by

$$P_p = F'_c A_p \quad (2)$$

where

- A_p = nominal cross-sectional area of the post
- F'_c = specified minimum compression stress of the timber blocking after applicable modification factors are applied (AFPA, 1996)

As the compression capacity in the bearing joint region is considered over a short length, the post stability factor in this calculation is equal to 1.0. It is noted that stability of the post should be considered as a separate limit state in the design of the post.

The strength of the joint region can then be determined from the interaction of the flange bending and post compressive strength using the following relationship

$$\left(\frac{P_u}{R_f}\right)^2 + \left(\frac{P_u}{P_p}\right)^2 \leq 1 \quad (3)$$

where

- P_u = applied axial load in the post

Bearing Area Method

This method focuses on the post capacity for calculating the ultimate load, with the impact of flange bending inherent but not explicitly considered in the formulation. The method is found to be more effective for a steel post where the post is axially rigid and thus does not allow the flange to deform before failure of the post, unlike a more flexible timber post (Carden et al., 2005). For this model an effective cross-sectional area of the steel post is considered to carry the entire axial load, as shown in Figure 3, and can be calculated using similar assumptions to those used in the web yielding equation given by the AISC Specification (AISC, 2005). The effective area of the post is determined by the width of the post that is effective in carrying the load multiplied by the thickness of the post walls. An equation for the capacity of a steel post is given by

$$P_p = \left[\alpha (t_f + t_{bp}) + 2k_1 \right] 2t_p F_{yp} \quad (4)$$

where

- α = constant which depends on the slope of the stress gradient assumed through the flange
- t_{bp} = thickness of the base plate of the post

- k_1 = distance from the center of the web to the edge of the fillet
- F_{yp} = specified minimum yield stress of the post
- t_p = wall thickness of the round hollow steel section

The $2t_p$ allows for the transfer of axial load on two sides of the round hollow steel post section.

Strength of Blocking

Falsework design typically avoids the use of stiffeners, as beams are reused and construction is temporary. However, in some cases timber blocking is used in an attempt to stiffen the beam flanges. Generally timber blocks sized between 4×4 in. and 6×8 in. are used, the capacity of which can be calculated based on the axial compression capacity of a short timber member. However, experimental and analytical studies showed that the full capacity of the blocking is generally not effective, particularly for a steel post, thus the capacity of the timber blocking, P_b , can be given by

$$P_b = \gamma F'_c A_b \quad (5)$$

where

- γ = blocking effectiveness factor
- A_b = combined cross-sectional area of the blocking on both sides of the web

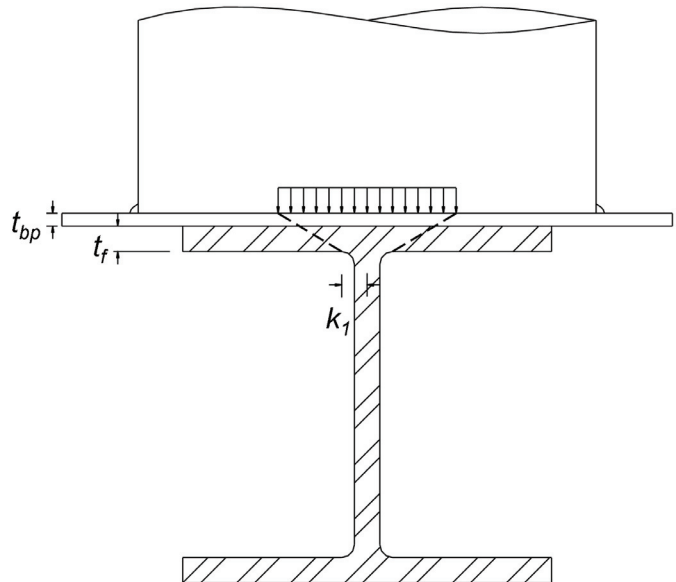


Fig. 3. Effective area of steel post for calculating the ultimate post load.

EXPERIMENTAL STUDIES

Experimental Setup

A series of experiments were performed to study different limit states in a flange-post bearing joint region. A total of 15 experiments focused on quantifying the flange-post joint capacity; 13 with timber posts and two with steel posts. The experimental setup with a timber post and steel beam is shown in Figure 4 as an example of one configuration. The flanges were restrained at the ends of the 48 in. long beam segments by the steel frame shown in the figure, preventing lateral instability of the beams for studying the flange and post limit states. Loads were applied to the end of the 48 in. long posts through a slider to limit lateral deformation at the end of the post, which was attached to a displacement controlled hydraulic actuator. The instrumentation consisted of displacement transducers and strain gages, as well as a machine-vision camera that allowed the measurement of strains and deformations. Three different beam sections were used, including ASTM A572 Gr. 50 HP12×53 and HP14×73 beams, and ASTM A992 W14×90 beams. Number 2 Douglas Fir 12 × 12 in. timber members were used for the posts and corbels. An 18-in.-diameter $\frac{3}{8}$ -in.-thick A500 Gr. B (42 ksi) round hollow steel section with a $\frac{1}{2}$ -in.-thick base plate was used to simulate a steel post. In some of the experiments, 6 × 8 in. Number 2 Douglas Fir timber blocking was also placed between the flanges on both sides of the web. The effects of eccentric patch loading were also investigated experimentally by introducing eccentricities ranging from $\frac{1}{12}$ to $\frac{1}{6}$ of the flange width. The failure load of the joints between the beams and steel posts could not be directly

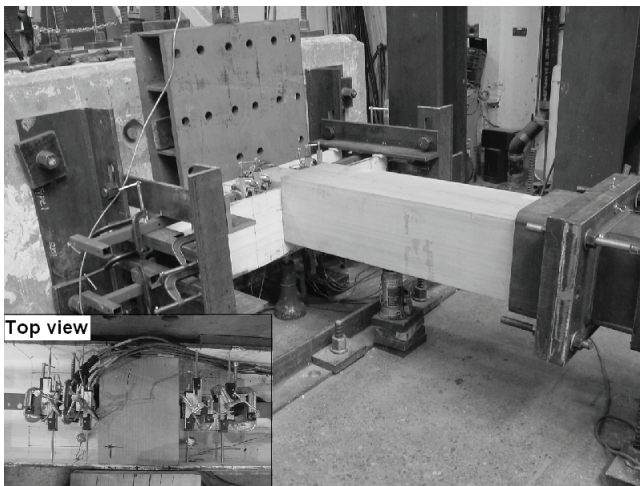
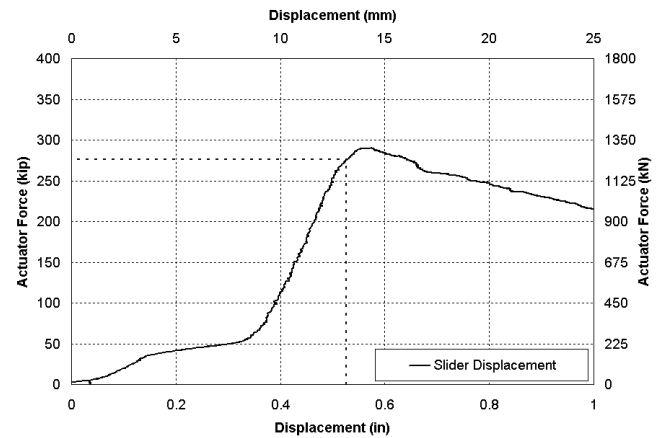


Fig. 4. Experimental setup with a timber post and steel beam with blocking and an eccentricity between the centroid of the beam and post.

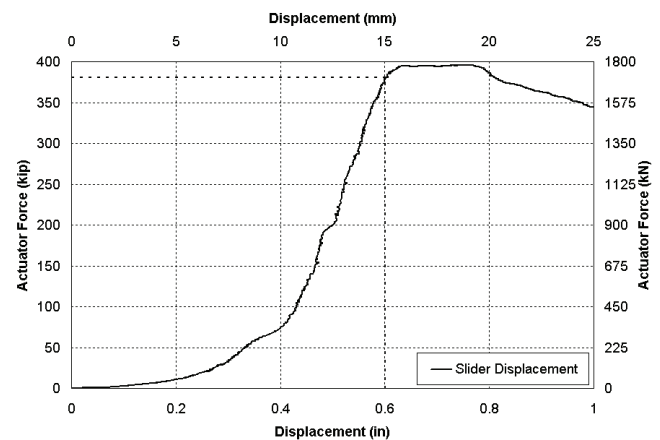
obtained from the two experiments, as timber corbels (members located under the sill beam in typical bridge falsework and located between the beam and reaction plate in experiments similar to that shown in Figure 4) were included in these experiments and governed the failure response.

Experimental Results

The force measured in the actuator was plotted against the axial displacement at the slider end of the post for each experiment. A typical force-displacement curve for a beam concentrically loaded through a timber post without any blocking is shown in Figure 5a, and that for a beam with blocking is shown in Figure 5b. These figures show that the stiffness initially increases as any gaps due to lack of fit between the



(a)



(b)

Fig. 5. Force displacement curve for HP14×73 beams: (a) concentrically loaded with no blocking and (b) concentrically loaded with blocking.

various components close, after which the maximum stiffness is reached. The stiffness decreases and load then starts to drop as crushing of the post and plastic deformation in the flange occurs. Comparison of Figures 5a and 5b shows that blocking resulted in slightly improved capacity.

The ultimate load was defined as the load at which the stiffness reduces to 50% of the initial stiffness, where the initial stiffness was defined as the stiffness between 25% and 75% of the ultimate load. Accordingly, the ultimate load, determined iteratively, is shown by the dashed lines in Figure 5 and is typically within 10% of the maximum load where post crushing and flange bending occurred.

A mixture of suspended lime and water was painted onto each beam and was observed to flake off once the steel started to yield. For each of the beams, the observed load where flaking occurred on the beam flange was recorded, with flaking typically located initially at the edge of the fillet between the flange and web under the post. Figure 6 compares the load at which flaking was observed with the estimated ultimate load based on the relative stiffness of the beams with timber posts. With the steel posts, flaking was not observed in the beams until after the posts had already yielded and thus is not included in the figure. Comparisons for different beam sizes and different configurations with and without blocking, and with different eccentricities between the post and beam are plotted in Figure 6. There are only 12 points for 13 experiments with timber posts as flaking was not observed at the appropriate time in one of the beams due to premature failure of the timber post. As can be seen in the figure, observed and estimated ultimate force is different by no more than 13% for each beam, with an average difference of 2%. The comparison therefore indicates that the estimated ultimate load, based on a 50% reduction in stiffness, is

similar to the load at which yielding is first observed, and thus, is an appropriately defined ultimate load.

Along with the subassembly experiments, component experiments were performed to determine the axial capacity of three timber posts, three timber blocks, and a steel post. The resulting axial capacity of the timber post, based on an average from the experiments, was 352 kips. The average axial capacity of the timber blocks was 163 kips and the capacity of the steel post was 888 kips. In addition, eight coupon tests were performed on samples of steel from the beams resulting in an average yield stress of 53 ksi and a range between 50 and 58 ksi.

For the beams with timber posts, the capacity of the flange-post joint region was calculated using Equations 1, 2, 3 and 5, when blocking was used, using the actual strengths of the post, blocking and steel material from the component experiments. Equation 1, with a β value of 18, was used to estimate the flange bending capacity. The timber blocking was assumed to be 100% effective, thus a γ value of 1.0 was assumed in Equation 5 and the effective blocking capacity was directly added to the flange bending capacity. The blocked or unblocked flange capacity was then combined with the timber post strength from Equation 2 using Equation 3. The experimental data show that there is a relatively small reduction in capacity when the post is eccentric to the centroid of the beam. Thus it is assumed that the above equations apply equally when there is an eccentricity equal to or less than $\frac{1}{6}$ of the width of the flange. The resulting calculated capacity of the flange-post region for the beams with timber posts is compared in Figure 7 to the estimated ultimate force from the experimental data, based on a 50% reduction in stiffness. The estimated forces are approximately equal to or less than the observed forces, at between 71% and 105% of

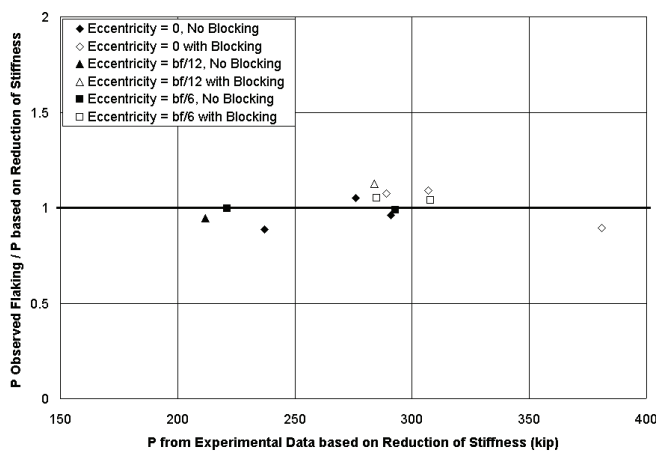


Fig. 6. Comparison of ultimate force observed due to flaking on the flange and ultimate force calculated at a 50% reduction in initial stiffness from force displacement curve.

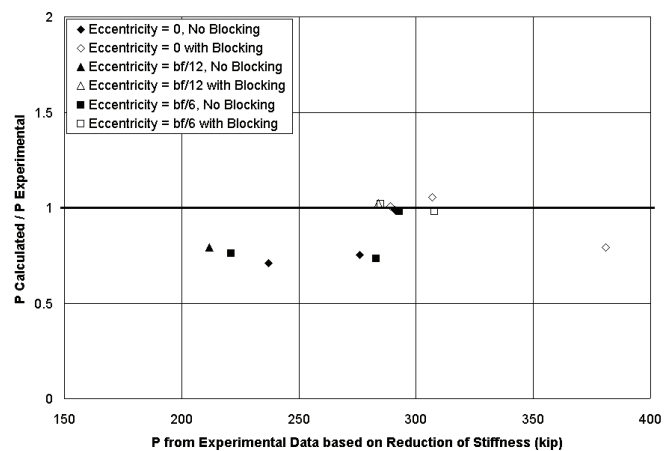


Fig. 7. Comparison of calculated ultimate force to experimental ultimate force based on a 50% reduction in stiffness.

that observed, for all members. The stagger in the observed capacities is mainly attributed to the variability of material properties, particularly for the timber members. The lime flaking pattern observed in the beams after considerable inelastic flange bending was very similar to the yield pattern assumed in developing Equation 1. Therefore, this method is appropriate for predicting the capacity of the flange-post joint region with a timber post.

The effective post bearing area method was used to estimate the capacity of the flange-post joint region with a steel post, based on Equation 4. The observed failure mode in the experiments with the steel post was consistent with the effective bearing area assumed for calculating the ultimate load, with yielding and crippling of the post occurring in the region where the post was bearing on the beam in line with the web. Unfortunately, the calculated ultimate load could not be directly compared to the experimental data as timber corbels were also used in experiments with the steel posts and these affected the ultimate load of the system. Thus, finite element analyses were used for comparison with the calculated ultimate load for cases with steel posts.

FINITE ELEMENT ANALYSES

Models

A series of finite element models of the different experimental configurations were developed and verified using the experimentally recorded response data. These finite element models allowed a larger range of beams and configurations to be considered, without material variability affecting the results. HP12×53, HP14×73, HP12×89 and W14×90 beams were modeled with timber posts (Figure 8a), and W14×90, HP14×117 and W14×120 beams were modeled with steel posts (Figure 8b).

The beams, posts and blocking were modeled with linear three-dimensional eight node elements in ABAQUS (Hibbett, Karlson and Sorensen, 2003), meshed typically as shown in Figure 8. The steel members were modeled with a plastic isotropic material using an expected yield strength of 55 ksi for the A572 Gr. 50 and A992 steel beams (approximately equal to the 53 ksi average strength measured from coupon tests) and 46 ksi for the A500 Gr. 42 steel posts. The timber posts were modeled with a multi-linear material model to fit the observed force-displacement relationships resulting from both material and geometric nonlinearities. Experiments on the 11.5 in. square Douglas Fir timber posts resulted in a calculated nominal post strength of 2.7 ksi, which was assumed as the first-yield stress in the finite element model. The stress was assumed to increase linearly by 20% to allow for material and geometric stiffening up to 2 times the yield strain. The stress was then assumed to gradually decrease to zero

at a strain of 10% to reflect the reduction in strength due to crushing. Based on measured values from experiments, the elastic modulus was equal to 550 ksi. The multi-linear model was found to compare better to the experimental data than pre-defined material models in ABAQUS. The 7.5 × 5.5 in. blocking elements were modeled with a similar model using a 4.0 ksi initial yield stress and a 330 ksi elastic modulus, as determined from the component experiments.

Loads were applied axially to the top of the post in displacement control until after the maximum load in the system was reached. The interfaces between the beams and other components were modeled with surfaces which are assumed to be connected by maintaining a constant geometric relationship between adjacent nodes. This is similar to a contact model with a high friction coefficient between nodes, but was found to be significantly more computationally efficient with comparable results. The nodes under the beams were completely restrained, while at the end of the post, the nodes were restrained to allow axial deformation only. Both flanges at the ends of the beam were also restrained to prevent out-of-plane deformation of the flanges.

For each configuration considered, the axial force in the post was plotted against the axial displacement at the free end of the post or patch load. The ultimate load was defined from the force-displacement curve at a point where the tangential stiffness reduced to 50% of the initial stiffness, consistent with the experimental data.

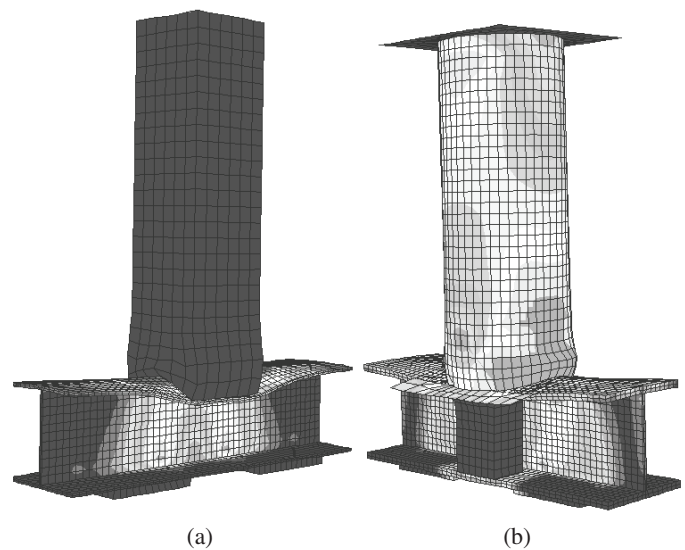
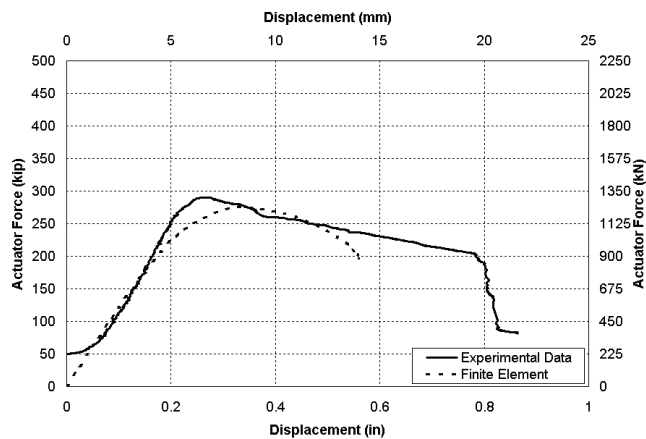


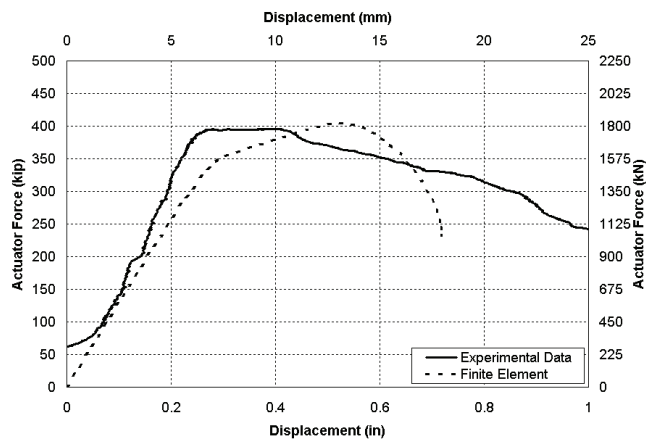
Fig. 8. Finite element models for: (a) a timber post and beam and (b) a steel post and beam with blocking.

Results from Analyses

Comparisons of the force-displacement curves from the finite element model and experimental data for two typical beams with and without blocking are shown in Figures 9a and 9b, respectively. The displacement from the experimental data was offset so that extrapolation of the maximum stiffness passed through the origin, to allow comparison with the finite element results. The comparisons show that the initial slope and maximum load were similar between the finite element and experimental models. A comparison between the ultimate loads calculated from the finite element model and experimental data is given in Figure 10. The load obtained from the finite element analysis is between 76% and 121%



(a)



(b)

Fig. 9 Comparison of force-displacement curve for HP14×73 beams: (a) concentrically loaded with no blocking and (b) concentrically loaded with blocking from experimental data and finite element analysis.

of the experimental load. Therefore, there is good correlation between the experimental and finite element results, with the variability attributed primarily to the variability in the capacity of the different posts and blocking.

The finite element results show that blocking resulted in a 20 to 70% increase in the flange-post joint capacity when using a timber post, depending on the flange bending capacity. With a steel post, blocking allowed only a 20 to 25% increase in the joint capacity. An eccentricity between the centroids of the flange and post equal to a maximum of $\frac{1}{6}$ of the flange width, resulted in a relatively small reduction in the flange-post capacity of 10 to 15% when using a timber post. With a steel post, each eccentric case resulted in an almost identical flange-post capacity to the concentric case.

The calculated flange-timber post capacity based on the interaction equation (Equation 3), as a ratio of the capacity calculated from the finite element analysis, is plotted in Figure 11a, for different beam sizes, with and without blocking and with different eccentricities. The blocking was considered to be 100% effective ($\gamma = 1.0$) with the timber posts, as described previously. Figure 11a shows that for the beams with timber posts, the calculated capacity is between 80% and 105% of the capacity calculated from the finite element model, with just two exceptions. These exceptions are for the larger beams with a large eccentricity where the calculated capacity is up to 119% of that from the finite element model. This level of eccentricity is unlikely to occur in a real situation; therefore, these cases are not of particular concern. Furthermore, when appropriate factors and nominal strengths instead of expected strengths are used in design, these cases are expected to be conservative as well. In practice, the maximum eccentricity should be limited to $\frac{1}{6}$ of

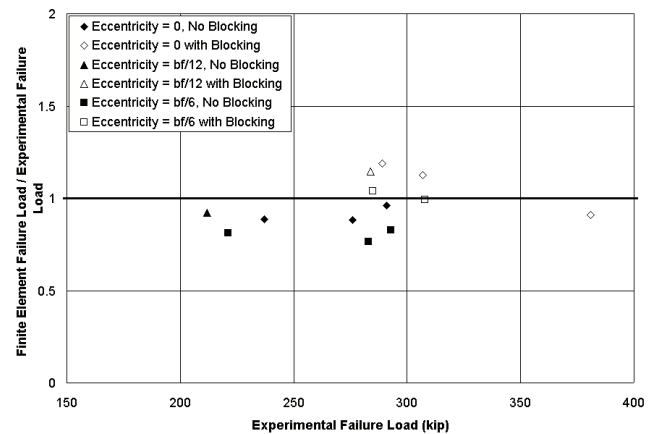


Fig. 10. Comparison of ultimate force from experimental data and finite element analysis.

the flange width. The calculated capacity based on the interaction equation appears to be relatively accurate and generally conservative for all cases including those with timber blocking.

With the steel posts, the ultimate capacity of the flange-post joint region is calculated using the effective bearing area method (Equation 4). As the stiffness of the post is greater than the stiffness of the blocking, the effectiveness of the blocking is reduced to 30% ($\gamma = 0.3$). While the blocking can be loaded further and the force carried by the joint continues to increase, significant flange bending and post yielding occurs resulting in significant permanent deformations in both beam and post. Thus, the effectiveness of timber blocking with a steel post is limited. Comparisons between the calculated capacity using the effective post bearing area and

effective blocking capacity (Equations 4 and 5) and the finite element analyses are shown in Figure 11b. The method is shown to be accurate and conservative, with calculated capacities between 81% and 105% of those from the finite element model. The use of a 30% effectiveness factor for the timber blocking gives a ratio of calculated to finite element capacity with the timber blocking relatively consistent to that without the timber blocking.

DESIGN OF FLANGE-POST BEARING JOINT REGIONS

Design Strength with a Timber Post

It is noted that the actual strength of the posts and beams were used in the comparisons discussed earlier. Clearly, the use of minimum specified stresses along with application of load factors and resistance factors for LRFD, or allowable stresses for ASD, will result in additional conservatism in the design equations. In LRFD format, for a steel beam with a patch load from a timber post, the factored applied load in the post, P_u , should be less than a combination of flange bending capacity, including blocking, and the post compression capacity for a short length of post, such that

$$P_u < \left(\frac{1}{\phi R_{nf}^2} + \frac{1}{\phi P_{np}^2} \right)^{-\frac{1}{2}} \quad (6a)$$

where

ϕR_{nf} = design strength of the flange including blocking

ϕP_{np} = design strength of the post

The design strength of the flange, including blocking (when used), is given by

$$\phi R_{nf} = \phi_b 18t_f^2 F_{yf} + \lambda \phi_c F_c' A_b \quad (6b)$$

where

ϕ_b = resistance factor for flange bending, equal to 0.90 (AISC, 2005)

ϕ_c = resistance factor for compression in the blocking, equal to 0.90 (AFPA, 1996)

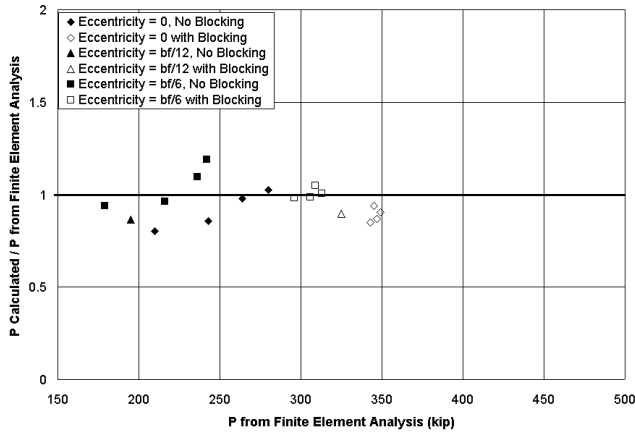
λ = time effect factor, equal to 1.0 for a typical falsework duration

The design strength of the post is given by

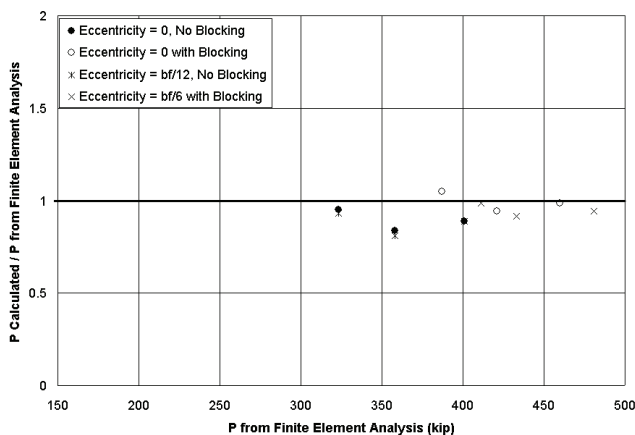
$$\phi P_{np} = \phi_c F_c' A_p \quad (6c)$$

where

ϕ_c = resistance factor for compression in the post, equal to 0.90



(a)



(b)

Fig. 11. Comparison of finite element analysis with calculated ultimate force using: (a) the interaction equation (Equation 3) and (b) the effective bearing area (Equation 4).

In ASD format, the applied stress in the post, f_c , should be less than the combination of allowable effective stress from flange bending capacity, F_{cf} , and allowable stress in the post, F'_{cp} , such that

$$f_c < \left(\frac{1}{F_{cf}^2} + \frac{1}{F_{cp}'^2} \right)^{-\frac{1}{2}} \quad (7a)$$

The effective stress from flange bending capacity, including the capacity provided by timber blocking, can be determined from

$$F_{cf} = \frac{18t_f^2 F_f}{A_p} + \frac{F'_{cb} A_b}{A_p} \quad (7b)$$

where

F_f = allowable flange stress, equal to 22 ksi for A36 steel or 30 ksi for A572 Gr. 50 or A992 steel beams if the allowable stress safety factor (1.67) is applied as defined by the *AISC Specification* (AISC, 2005)

F'_{cb} = allowable compression stress in the timber blocking (AFPA, 2001)

F'_{cp} = allowable stress in the post, due to post compression over a short length of the post, with applicable modification factors, is taken directly from the ASD specifications (AFPA, 2001)

Design Strength with a Steel Post

The design capacity of the flange-post bearing joint region with a steel post can be most accurately determined using the effective bearing area. Therefore, using the LRFD format, design of the flange-post region should ensure that

$$P_u < \phi R_n \quad (8a)$$

where

P_u = factored applied load

ϕR_n = design strength of the post in bearing, including the strength provided by blocking

ϕR_n is given by

$$\phi R_n = \phi_{cp} \left[5(t_f + t_{bp}) + 2k_1 \right] 2t_p F_{yp} + \phi_{cb} 0.3F'_{cb} A_b \quad (8b)$$

where

ϕ_{cp} = resistance factor for compression in the post, which, to be consistent with that used for web yielding, equal to 1.00 (AISC, 2005)

ϕ_{cb} = resistance factor for the blocking, equal to 0.90

In ASD format the flange-post connection region for a steel post should be designed such that

$$f_{cp} < F'_{cpb} \quad (9a)$$

where

f_{cp} = applied compression stress in the gross cross-sectional area of the post

$$f_{cp} = \frac{R}{\left[5(t_f + t_{bp}) + 2k_1 \right] 2t_p} \quad (9b)$$

where

R = applied force in the post

The allowable stress in the post including blocking is given by

$$F_{cpb} = F_{cp} \left(1 + \frac{0.3F'_{cb} A_b}{F_{cp} \left[5(t_f + t_{bp}) + 2k_1 \right] 2t_p} \right) \quad (9c)$$

where

F_{cp} = 28 ksi for an A500 Gr. B round hollow steel section based on an allowable stress safety factor of 1.50, as for web yielding (AISC, 2005)

F'_{cb} = allowable stress in the timber blocking (AFPA, 2001)

SUMMARY AND CONCLUSIONS

The capacity of the beam-post joint region for an unstiffened beam supporting or supported by a timber or steel post, similar to those found in bridge falsework, may be governed by a combination of flange bending and post crushing or yielding. A series of experiments and finite element analyses were conducted to investigate potential failure mechanisms and to quantify the flange-post joint capacity. Also considered in the study was the effect of: i) blocking placed between the top and bottom flanges, and ii) eccentricity between the centroids of the beam and post. Accordingly, the following observations were made:

1. The ultimate capacity of the joint is defined at a point where the stiffness of the force-displacement curve reduces to 50% of the initial stiffness. This definition of the ultimate capacity provided consistent correlation with the experimental observations; namely onset of flange bending.
2. Depending on the size of the beam, timber blocking is found to increase flange-post joint capacity by 20 to 70%.

3. When used under a steel post with large beam sections, timber blocking is less effective resulting in a maximum likely increase of 25% in joint capacity.
4. An eccentricity between the flange and a timber post, which should be limited to 1/4 of the flange width results in a reduction of flange-post strength of 10 to 15%.
5. The effect of eccentricity, which should be limited to 1/4 of the flange width, on the joint capacity when steel posts are used is negligible.

Two methods were developed for predicting the flange-post joint capacity; namely, the interaction method and the effective bearing area method. The interaction method accounted for a combination of flange bending and post crushing capacities. Based on the experimental and analytical observations, this method is found appropriate and recommended for use in calculating the capacity of joints that consist of a timber post bearing onto a beam flange. Blocking can be considered “100% effective” ($\gamma = 1.0$ in Equations 5 and 7b) with respect to increasing the flange bending capacity when a timber post is used. The effective bearing area method is recommended for calculating the flange-post joint capacity with a steel post and is derived based on assumptions similar to those used in the calculation of web yielding capacity. It is noted that timber blocking has a relatively low stiffness when used under a steel post. Therefore, a blocking effectiveness factor of 30% ($\gamma = 0.3$ in Equation 5) is recommended based on the experimental and analytical findings. Finally, design equations are presented in both LRFD and ASD format for calculating flange-post capacity with and without blocking.

ACKNOWLEDGMENTS

The authors would like to extend their gratitude to the California Department for Transportation for funding of this study under contract number 59A0445, with special thanks to John Lammers and Peter Lee for their assistance and direction.

REFERENCES

- AFPA (1996), *Load and Resistance Factor Design – Manual for Engineered Wood Construction*, American Forest and Paper Association, Washington, DC.
- AFPA (2001), *National Design Specification for Wood Construction*, American Forest and Paper Association, Washington, DC.
- AISC (2005), *Specification for Structural Steel Buildings*, American Institute of Steel Construction, Inc., Chicago, IL.
- Carden, L.P., Pekcan, G. and Itani, A.M. (2005), “Recommendations for the Design of Beams and Posts in Bridge Falsework,” *Research Report CCEER 05-15*, Center for Civil and Earthquake Engineering Research, University of Nevada, Reno, NV.
- Elgaaly, M. (1983), “Web Design Under Compressive Edge Loads,” *Engineering Journal*, AISC, 4th quarter, pp. 153–171.
- Graciano, C. and Edlund, B. (2003), “Failure Mechanism of Slender Girder Webs with a Longitudinal Stiffener under Patch Loading,” *Journal of Constructional Steel Research*, Vol. 59, No. 1, pp. 27–45.
- Graham, J.D., Sherbourne, A.N. and Khabbaz, R.N. (1959), *Welded Interior Beam-to-Column Connections*, American Iron and Steel Institute, Inc., Chicago, IL.
- Hibbett, Karlson and Sorensen, Inc. (2003), “ABAQUS – Finite Element Program,” Hibbett, Karlson & Sorensen, Inc., Fremont, CA.
- Roberts, T.M. and Markovic, N. (1983), “Stocky Plate Girders Subjected to Edge Loading,” *Proc. Instn. Civ. Engrs.*, Vol. 75, No. 2, pp. 539–550.
- Roberts, T.M. and Newark, A.C.B. (1997), “Strength of Webs Subjected to Compressive Edge Loading,” *Journal of Structural Engineering*, Vol. 123, No. 2, pp. 176–183.
- Roberts, T.M. and Rockey, K.C. (1979), “A Mechanism Solution for Predicting the Collapse Loads for Slender Plate Girders when Subjected to In-Plane Patch Loading,” *Proc. Instn. Civ. Engrs.*, Vol. 67, No. 2, pp. 155–175.
- Shahabian, F. and Roberts, T.M. (1999), “Buckling of Slender Web Plates Subjected to Combinations of In-Plane Loading,” *Journal of Constructional Steel Research*, Vol. 51, No. 2, pp. 99–121.